EXPERIMENTAL FLUTTER INVESTIGATIONS OF AN ANNULAR COMPRESSOR CASCADE: INFLUENCE OF REDUCED FREQUENCY ON STABILITY

Joachim Belz and Holger Hennings
DLR – Institute of Aeroelasticity
Bunsenstrasse 10
D-37073 Göttingen, Germany
joachim.belz@dlr.de
holger.hennings@dlr.de

Abstract Due to the trend of increasing power and reducing weight, the fan and compressor bladings of turbomachinery might be more sensitive to flutter, which must strictly be avoided already in the design process. In order to increase our understanding of the flutter phenomena for fan and compressor cascades, aeroelastic investigations are essential.

This paper presents the achievements and results of experimental flutter investigations with a compressor cascade in the test facility of non-rotating annular cascades at EPFL. Flow conditions such as those that occur in rotating cascades are simulated by generating a spiral flow in the upstream. The construction of the cascade which takes into account the structural properties necessary to perform flutter experiments is described. For the simulation of elastic torsional vibrations of a two-dimensional blade section, the cascade consists of 20 blades (NACA3506 profile) mounted on elastic spring suspensions which allows for torsional motion about the midchord.

In order to investigate the influence of the reduced frequency on the global stability of the cascade and its local contibutions, experiments were performed for two different reduced frequencies. At the higher reduced frequency the cascade remains aerodynamically stable, however, at the lower reduced frequency and transonic flow conditions, some of the interblade phase angles appear to be aerodynamically unstable.

Keywords: Flutter, Reduced Frequency, Experiments, Annular Cascade

K.C. Hall et al.(eds.),
Unsteady Aerodynamics, Aeroacoustics and Aeroelasticity of Turbomachines, 77–91.

Introduction

The demand for a decrease in engine weight and a reduction in fuel consumption has, among other things, led to engines that contain a decreased number of compressor stages and slender fan or compressor blades. This results in both more flexible blades and in higher pressure ratios at each stage with a higher flow velocity around the blades. The variations of these parameters influence the aeroelastic stability of the blade assembly and can lead to flutter, i.e. self-excited blade vibrations due to an interaction with the motion-induced unsteady aerodynamic forces. For this reason, aeroelastic investigations are essential to provide detailed knowledge about flutter phenomena, especially for compressor cascades in transonic flow. Experimental data of unsteady aerodynamic and flutter tests are required for the validation of theoretical results as well.

In the past years, the increasing number of theoretical investigations has been accompanied by several experiments on vibrating cascades. Széchényi et al. (1980), Carta (1982), Buffum et al. (1998), and Lepicovski et al. (2002) have obtained unsteady aerodynamic data by harmonic torsional oscillations of one blade or all blades of their linear compressor cascades. Carta particularly showed the influence of the interblade phase angle on stability at low Mach numbers, whereas Széchényi and Buffum concentrated their investigations on the influence of large incidence angles on stability. Körbächer (1996) investigated the bending motion of the blades of a compressor cascade in an annular wind tunnel. A cascade with the same geometry was used by Hennings and Belz (1999, 2000) to examine the aerodynamic damping by forced pitching motions of the blades with respect to shock movements. The results were compared with theoretical investigations by Carstens and Schmitt (1999) as well as Kahl and Hennings (2000), who took into account leakage flow effects.

The experimental investigations presented here were performed in the wind tunnel for annular cascades at the École Polytechnique Fédérale de Lausanne (EPFL). This wind tunnel has been used by several other researchers for the measuring of unsteady pressure distributions due to blade vibrations for aerodynamic stability investigations of compressor and turbine cascades or upstream generated aerodynamics gusts for forced response investigations. The following investigations performed are cited as examples: Körbächer and Bölcs (1996), Körbächer (1996), Nowinski and Panovsky (1998)), Rottmeier (2003).

The aim of the investigation presented here was to investigate the influence of reduced frequencies on the cascade's aerodynamic and aeroelastic behavior at transonic flow. Two reduced frequencies were chosen in such a manner, that in one case self-excited cascade vibration (flutter) occured and in the other case the cascade remained aerodynamically stable. In order to realize cascade flutter the structural damping had to be minimized by redesigning the elastic

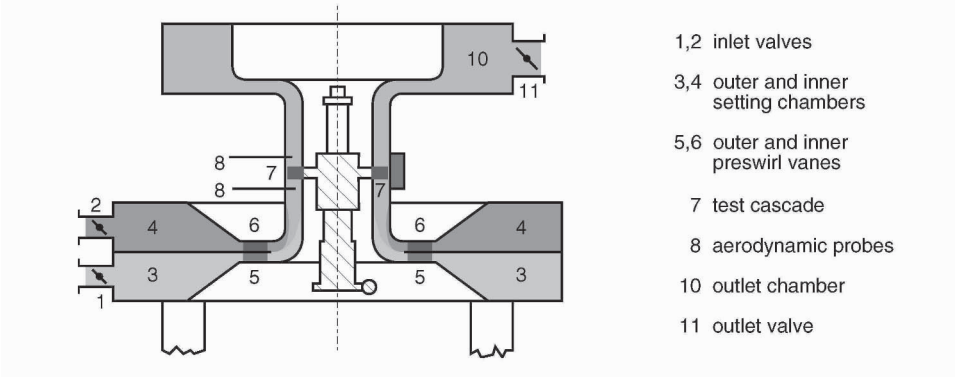

Figure 1. Schematic cross-section of the annular cascade tunnel; Bölcs (1983)

spring suspensions. The unsteady pressure distribution, the influence of the shock impulse at transonic flow conditions, and the local and global stability measured for the two reduced frequencies are compared.

1. Annular Test Facility

1.1 Annular Wind Tunnel

The experimental investigations presented here were performed in the wind tunnel for annular cascades at the EPFL. The annular cascade tunnel was developed for a research project between BBC and the EPFL to investigated the steady and unsteady flow in annular cascades without having to rotate them; Bölcs (1983). A spiral flow is generated in order to simulate real inflow angles such as those that would occur in a rotating cascade. Figure 1 shows the cross-section of the wind tunnel. The advantage of an annular cascade such as circumferential flow periodicity is combined with the advantage of a fixed cascade in respect of data aquisition and data transfer. Steady flow conditions are measured by aerodynamic probes in the upstream and downstream sections and by pressure taps on the blades' surfaces. The aerodynamic probes were calibrated to obtain the total pressure p_{t_1} and p_{t_2}, the steady pressures p_1 and p_2, the flow angles β_1 and β_2, and the Mach numbers Ma_1 and Ma_2 from the measured pressure data.

1.2 Cascade

The compressor cascade used here is composed of 20 blades with a NACA 3506 profile of $c = 80\,\mathrm{mm}$ in nominal chord length, a stagger angle of $\beta_g = 40°$, and a pitch at midspan of $s = 56.5\,\mathrm{mm}$ (Fig. 2). The profiles were shortened to a $c_{\mathrm{red}} = 77.5\,\mathrm{mm}$ chord length with a round trailing edge (see

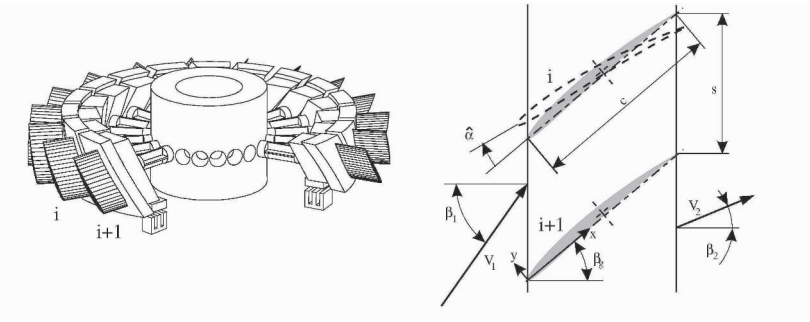

Figure 2. Components and geometry of the cascade

also Fig. 5 and 6). The blades are mounted via elastic spring suspensions which allow a torsional motion around midchord.

A NACA3506 profile was chosen for the investigations of tuned bending vibrations by Körbächer (1996). The fact that pitching motions of this profile should be more critical in aeroelastic stability – mainly for transonic flow conditions – was the reason why investigations of the aerodynamic damping using excited pitching vibrations were carried out by Hennings and Belz (1999, 2000). For the flutter measurements the blades are tuned to lower eigenfrequencies in order to reach an aerodynamically as well as aeroelastically unstable case. For the latter one the aerodynamic self-excitation has to surpass the structural damping of the cascade, namely of the elastic spring suspension.

For experimental investigations concerning the aerodynamic damping, the blades are driven by electromagnetic exciters such that their motions represent a traveling wave modes with one of the possible interblade phase angles

$$\sigma_k = \frac{2\pi}{N}\,(k-1) \quad , \quad k = 1...N \;, \tag{1}$$

given by the number of $N = 20$ blades. The unsteady pitching motions

$$\alpha_i(t) = \hat{\alpha} \cdot \cos(\Omega t - i\,\sigma_k) \tag{2}$$

of the blades are controlled in both their amplitudes $\hat{\alpha}$ and interblade phase angles σ_k. In order to reach appropriate amplitudes, the inertia of each blade and the vibrating part of the inner wall of the wind tunnel had to be reduced and the blades had to be excited near resonance (Figure 3 shows the assembly of the cascade). Lowering the eigenfrequencies by a minor mass moment of inertia, the torsional stiffness had to be reduced as well. So, the demand of both lower torsional stiffness (in presence of a high transversal stiffness to avoid a heaving motion) and lower structural damping led to a new one-piece spring suspension.

The spring suspension was made out a cylindrical part by cutting sections out using electrical discharge machining. The remaining section consists of

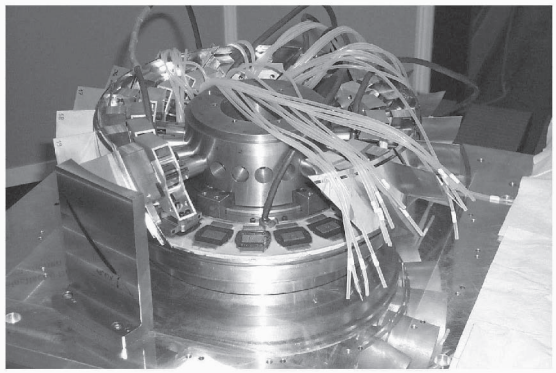

Figure 3. Annular cascade with some blades removed

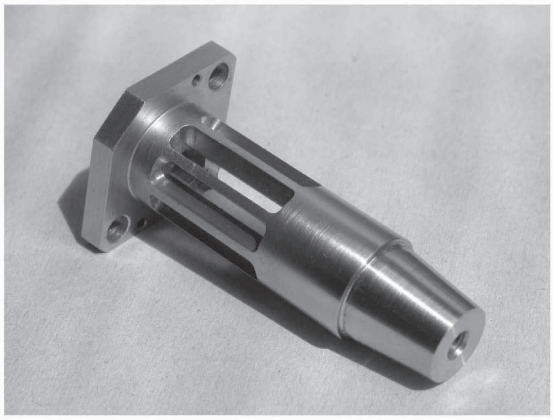

Figure 4. Elastic spring suspension

eight rectangular beams orientated such that the torsional stiffness is low and the transverse stiffness is high. The use of electrical discharge machining made it possible to manufacture the spring suspension out of one part, which results in a very low structural damping (see Figure 4).

2. Experimental Investigations

As blade flutter in axial turbomachines is caused by an interaction of the blade motions and the motion-induced unsteady aerodynamic forces, the main parameters for flutter beside the cascade's geometry and structural properties are the flow conditions and the damping properties of the structure. Hence, two different approaches for experimental flutter investigations are possible: in the so-called "aerodynamic approach" a certain level of structural damping is needed for the blades to prevent self-excited vibrations if the cascade

is aerodynamically unstable. In order to determine the aerodynamic damping the blades are forced into controlled harmonic vibrations in each traveling wave mode successively and the motion induced unsteady pressure distributions is measured. The analysis of this data — in particular the out-of-phase unsteady harmonic pressure — leads to an estimation of the aerodynamic stability of each traveling wave mode. In a so-called "aeroelastic approach" the aerodynamic instability can overcome for the structural damping and the cascade starts to flutter. With the use of some safety devices (like hydaulic flutter brakes), the blade vibrations and the unsteady pressure distributions can be measured at the onset of flutter.

In order to drive the cascade into flutter each blade was tuned to a lower eigenfrequency of $183\,\mathrm{Hz}$ by increasing the mass moment of inertia. This cascade was mounted in the annular wind tunnel. Steady flow conditions were achieved by adjusting the inlet total pressure, the inlet inflow angle, and the back pressure. A hydraulic brake prevented blade vibrations during the adjustment of the steady flow. These flow conditions were surveyed by probe measurements of upstream and downstream flow field and by measuring the steady pressure distribution on the blades.

At the up- and down-stream flow field an aerodynamic probe was used to scan one pitch of the cascade by taking small steps in the radial and circumferential directions. The measured probe pressures were used to compute mass flow averaged in- and out-flow values such as p_{t_1}, p_{t_2}, p_1, p_2, etc. (Table 1). The steady pressure distribution the blades were measured with pressure taps on the pressure and suction surface at nine equidistant chordwise positions and the three radial positions $z/h = 0.2, 0.5$, and 0.8 on several blades. They were transformed to steady pressure coefficients

$$C_p = \frac{p - p_1}{p_{t_1} - p_1} \tag{3}$$

using the mass flow averaged values of the inflow total and steady pressure p_{t_1} and p_1, respectively (Fig. 5).

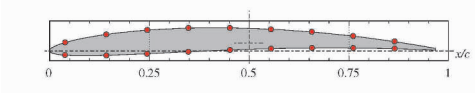

Figure 5. Location of the pressure taps

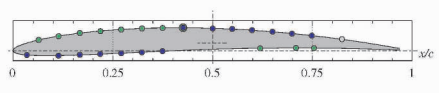

Figure 6. Location of the piezoelectric pressure transducers

Afterwards, the hydaulic brake was released to set the blade assembly to controlled pitching oscillations for the performance of the unsteady measurements ("aerodynamic approach") or to allow self-excited vibrations for the performance of the flutter experiments ("aeroelastic approach"). The unsteady pressure distribution was measured by 25 piezoelectric transducers, 15 of which

are mounted on the suction side and 10 on the pressure side of the blades. The transducers were distributed in blocks on only four blades. In each block, the transducers are located close together in order to resolve the unsteady pressure distribution near possible shock positions (Fig. 6).

The blade vibrations were measured by an eddy-current displacement sensor for each blade.

2.1 Investigated Flow Cases

The aim of the experiments was to investigate the behavior of a cascade running into flutter. In order to decrease the reduced frequency

$$\omega^* = 2\pi \, \frac{f \, c_{\mathrm{red}}}{v_1} \tag{4}$$

with respect to the same inflow velocity v_1 the cascade was tuned to a lower torsional blade eigenfrequency. So it was possible to investigate an unstable aeroelastic condition at a transonic flow case, which had been previously investigated.

Table 1. Steady upstream and downstream flow parameters

	Transonic Reference Case		Flutter Case	
ω^*	0.362		0.289	
	Upstream:	Downstream:	Upstream:	Downstream:
Ma	0.87	0.72	0.90	0.75
β	50.3 °	41.5 °	50.4 °	40.1 °
p_t	1323 mbar	1254 mbar	1397 mbar	1311 mbar
p	814 mbar	854 mbar	836 mbar	834 mbar

The transonic flow condition is characterized by the occurrence of a front shock at $x/c \approx 0.25...0.35$ and a channel shock at $x/c \approx 0.65...0.85$ on the suction side and at $x/c \approx 0.25...0.35$ on the pressure side (Fig. 7b). In- and out-flow parameters are mentioned in Table 1. Releasing the hydraulic brake at this flow condition, it was possible to set the blade assembly to controlled pitching oscillations around midchord for each interblade phase angle and to measure the unsteady pressure distribution up to a pitching amplitude of approximate $0.1°$ in order to determine the aerodynamic damping following the "aerodynamic approach". The excitation frequency of $177\,\mathrm{Hz}$ was choosen slighly below the eigenfrequency of the blades in order to distuinguish forced and free vibrations in the frequency range. This excitation frequency corresponds to a reduced frequency $\omega^* = 0.289$. Exceeding this amplitude the cascade starts to vibrate with a frequency of $182\,\mathrm{Hz}$ ("Flutter Case" Table 1).

With the same cascade, an aerodynamic damping investigations was performed following the "aerodynamic approach" with each blade tuned to a higher eigenfrequency and excited at $215\,\mathrm{Hz}$ ($\omega^* = 0.362$). Here the cascade remained aerodynamically and aeroelastically stable ("Transonic Reference Case" Table 1).

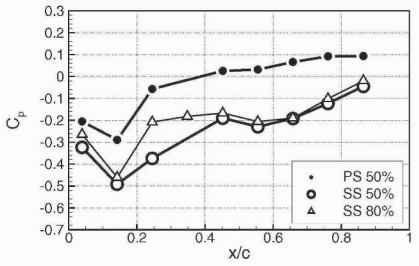

Figure 7a. Steady pressure distribution (C_p) of the transonic ref. case ($\omega^* = 0.362$)

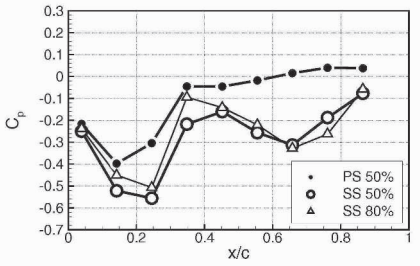

Figure 7b. Steady pressure distribution (C_p) of the flutter case ($\omega^* = 0.289$)

2.2 Evaluation of the Aerodynamic Damping

Due to the fact that the cascade in the "flutter case" remains aeroelastically stable for very small pitching amplitudes (below $0.2°$) it was possible to obtain unsteady pressure distributions caused by forced pitching vibrations of the blades in each traveling wave mode — in the same manner as the larger amplitudes in the "transonic reference case".

Following the "aerodynamic aproach" the measured unsteady pressure values and vibration signals were recorded. A Fourier transformation yields the first harmonic of the pressure which is related to the pitching motion of that blade i according to eq. (2) by

$$p(t) = \hat{p}\ \cos(\Omega t - i\,\sigma_k + \Phi)\ . \tag{5}$$

The unsteady pressure coefficient is defined as

$$\tilde{C}_p = \frac{\tilde{p}}{\hat{\alpha}\,(p_{t_1} - p_1)} \tag{6}$$

where $\tilde{p} = \hat{p}\,\exp(j\Phi)$ is the first harmonic of the unsteady pressure. The $\tilde{C}_p$-distribution for the interblade phase angle (IBPA) $\sigma_k = 72°$ is shown in Figure 8a for the "transonic reference case" and in Figure 8b for the "flutter case". In order to avoid numerical inaccuracies due to the discrete Fourier transformation, the sinusoidal vibration signals were Fourier transformed as

$\omega^* = 0.362$ $\omega^* = 0.289$

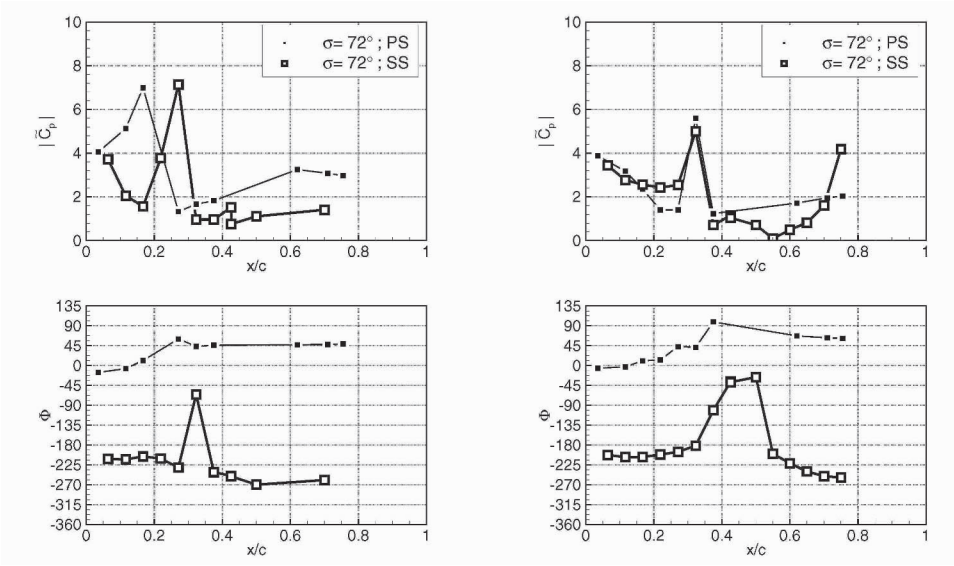

Figure 8a. Unsteady pressure coefficient $\tilde{C}_p$ for the IBPA $\sigma_k = 72°$ of the transonic reference case (magnitude at the top, phase at the bottom)

Figure 8b. Unsteady pressure coefficient $\tilde{C}_p$ for the IBPA $\sigma_k = 72°$ of the flutter case (magnitude at the top, phase at the bottom)

well. Arranging the $\tilde{C}_p$-distributions of each IBPA side by side, Figures 9a and 9b are obtained.

It can be seen from the pressure distribution of both cases, that the impulse response of the front shock is visible on the suction side at $x/c \approx 0.28$ in the "transonic reference case" and at $x/c \approx 0.32$ in the "flutter case". Comparing the channel shock of the "transonic reference case" with the "flutter case", the impulse response on the pressure side is visible at $x/c \approx 0.17$ in the "transonic reference case" and at $x/c \approx 0.32$ in the "flutter case". The impulse response of the channel shock is only visible at the suction side at $x/c > 0.75$ for the "flutter case".

The contribution of the locally acting aerodynamic forces due to the unsteady pressure to the aerodynamic damping of the cascade is given by the local work coefficient, i.e. the dimensionless work per unit arc length performed by the fluid on the blades. It is obtained by the integration with respect to time t over one period T of the pitching motion $\alpha(t)$ and yields

$$w^*(\xi) = \int_0^T \tilde{C}_p(\xi, t)\, \frac{\dot{\alpha}(t)}{\hat{\alpha}} \left[(\vec{r}(\xi) - \vec{r}_0) \times \vec{n}(\xi) \right]_3 \mathrm{d}t \tag{7}$$

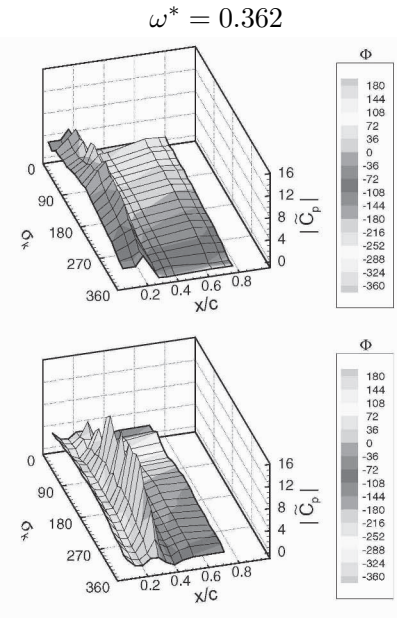

Figure 9a. Unsteady pressure coefficient $\tilde{C}_p$ for all IBPAs of the transonic ref. case (top: pressure side, bottom: suction side)

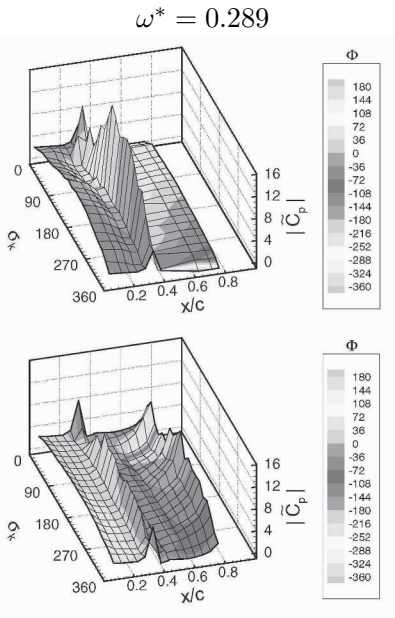

Figure 9b. Unsteady pressure coefficient $\tilde{C}_p$ for all IBPAs of the flutter case (top: pressure side, bottom: suction side)

where $(\vec{r}(\xi) - \vec{r}_0)$ is the dimensionless vector from the pitching axis to a surface point at the dimensionless arc length ξ and $\vec{n}(\xi)$ as the outward normal vector on that surface point. The subscript "3" denotes the radial component of the cross product. For the pitching motions of rigid blades in a given traveling wave mode, the local work coefficient is dependend on the amplitude of the aerodynamic moment due to the first harmonic of the unsteady pressure on a surface location, the (harmonic) pitching motion of that blade, and the phase between them to a local stability parameter. It is negative for stable and positive for unstable aerodynamic conditions.

In order to assess the aerodynamic stability of the two transonic cases in detail, the local work coefficient $w^*(\xi)$ is used to acquire an insight into the local contributions of the unsteady pressure at each measuring location — especially at locations, where considerable pressure fluctuations appear due to the shock movement, which is caused by the blade vibration. Regarding Figure 10a for the "transonic reference case" and Figure 10b for the "flutter case", the following aspects are recognizable:

- The contribution of the high unsteady pressure level on the leading edge stabilizes the pitching motion of the blade for all traveling wave modes. On the suction side, the local work coefficient is nearly constant, on

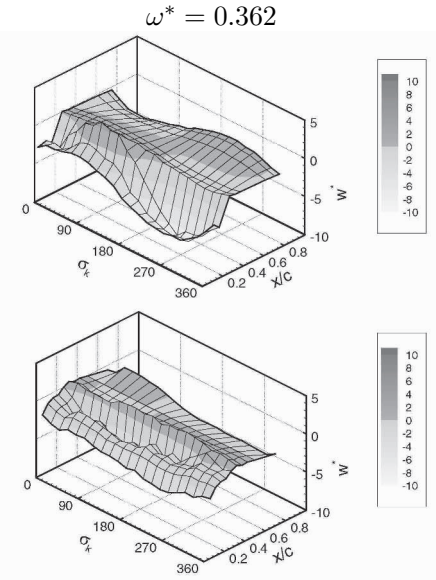

Figure 10a. Local work coefficient for all IBPAs of the transonic reference case (top: pressure side, bottom: suction side)

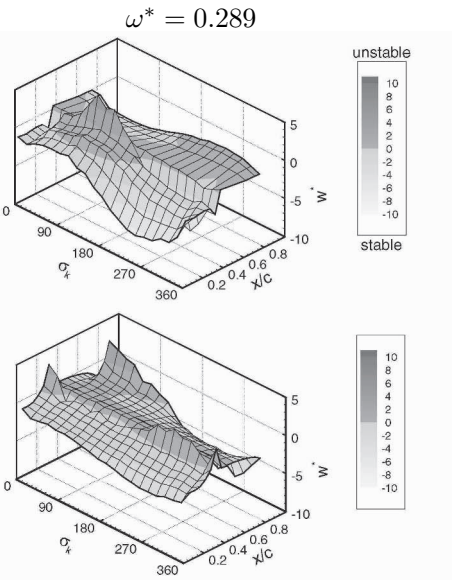

Figure 10b. Local work coefficient for all IBPAs of the flutter case (top: pressure side, bottom: suction side)

the pressure side, the stabilizing effect of the leadling edge for traveling wave modes with an IBPA between $180°$ and $360°$ is higher then for IBPA between $0°$ and $180°$.

- The high unsteady pressure level due to the front shock is stabilizing the motion in all travelling wave modes except for those with an IBPA between $288°$ and $360°$ for the "transonic reference case". Here the local work coefficient is near zero, that means no significant contribution to stability or instability. In contrast to that, the shock impulse of the front shock stabilizes only for the IBPA between $36°$ and $180°$ in the "flutter case" — for the other traveling wave modes it destabilizes.

- Comparing the channel shock impulse on the pressure side, in both cases the largest contribution to instability occurs in the vicinity of an IBPA of $126°$, but at a higher level for the "flutter case" Regarding the contribution of the front shock impulse on the suction side, this effects may cancel each other out.

- The most significant difference between the two cases is the strong channel shock impulse on the suction side in the "flutter case". Due to its

position near trailing edge and the large moment arm, its contribution is very strong:

- to the stability for the IBPAs between $180°$ and $360°$ and between $0°$ and $18°$
- and to the instability for the IBPAs between $36°$ and $162°$ with a strong jump between stability at $18°$ and instability at $36°$.

In order to assess how these contributions affect the flutter behavior of the cascade, a global damping parameter was evaluated as follows: With the definition of the unsteady pressure coefficient according to eq. (6), the unsteady moment coefficient $\tilde{C}_M$ is calculated. Using the imaginary part, the global damping coefficient is defined as

$$\Xi = -\operatorname{Im}\{\tilde{C}_M\} = +\operatorname{Im}\left\{\int_0^{S/c} \tilde{C}_p(\xi)\left[(\vec{r}(\xi)-\vec{r}_0)\times\vec{n}(\xi)\right]_3 \mathrm{d}s\right\} . \quad (8)$$

A positive value of Ξ represents stability with damped oscillations; negative values indicate instability.

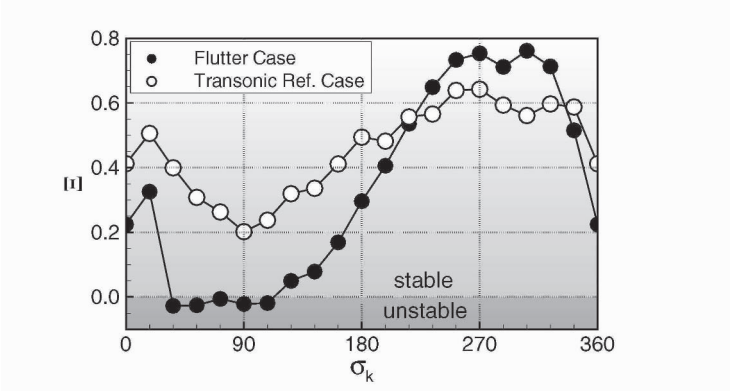

Figure 11. Global damping coefficient Ξ of the "flutter case" (black) and the "transonic referece case" (white)

It can be seen, that in both cases the traveling wave modes with the lowest aerodynamic damping occur at IBPA near $90°$. Especially for the flutter case, the aerodynamic damping for IBPA between $36°$ and $108°$ is negative, i.e. if the structural damping could not compensate this aerodynamic instability, the cascade starts to flutter.

2.3 Flutter Measurements

Increasing the vibration amplitude beyond a certain level in the "flutter case" the cascade starts with self-excited vibrations. Figure 12 plots the amplitude

of some blades versus time when the cascade was excited at a frequency of $177\,\mathrm{Hz}$. After reaching a certain amplitude, the cascade start to vibrate at its eigenfrequency of $182\,\mathrm{Hz}$. Then the excitation was turned down. While the cascade was vibrating in its eigenfrequency and was simultaneously excited, beats are clearly visible. A Fourier analysis performed every $100\,\mathrm{ms}$

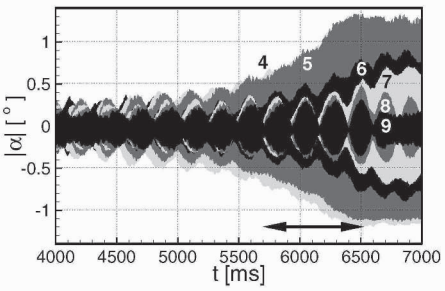

Figure 12. Increasing amplitudes of the blades 4 ... 9 of the flutter case

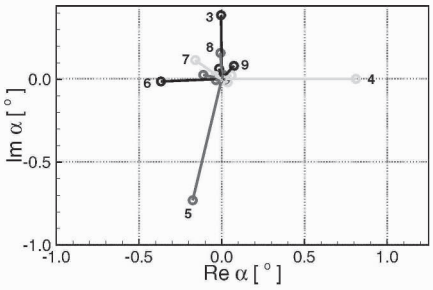

Figure 13. Amplitudes and phases of the blade deflections at $t = 5700\,\mathrm{ms}$

for sections of $819\,\mathrm{ms}$ (8192 time samples) leads to the complex amplitudes (amplitude and phase) and gives an insight into the vibration mode. (Figure 13 shows the results of a Fourier analysis started at $5700\,\mathrm{ms}$.)

It is visible, that only some blades — namely blade 3 to 9 — were vibrating with a significant amplitude. The phase between these blades remained constant over time, but there is no equal interblade phase angle between all blades visible. This may be caused by the cascades's mistuning due to blades equiped with pressure taps and tubes as well as blades with unsteady pressure transducers.

3. Summary

Measurements of aerodynamic damping were performed for nearly identical transonic flow cases, but for different reduced frequencies. For the lower reduced frequency the cascade was proven to be aerodynamically unstable. Besides the front shock impulse and pressure side's channel shock impulse this unstable case was characterized by a strong channel shock impulse near suction side's trailing edge. While the effects of the front shock impulse and pressure side's channel shock impulse canceled out each other, the impulse of the channel shock near the trailing edge on the suction side had a significant influence on stability. Increasing the forced vibration amplitude, the cascade started with self-excited vibrations.

Acknowledgments

The investigations were carried out as part of a joint research project of the MTU Aero Engines GmbH and the DLR Institute of Aeroelasticity. The authors would like to acknowledge the authorization for publishing the results here. They would also like to extend their thanks to Prof. Bölcs (EPFL) for the possibility of using the annular wind tunnel. Finally, the technical support by Mr. Beretta, Dr. Ott, and Dr. Rottmeier is gratefully acknowledged.

References

Belz, J., Hennings, H. (2000). *Aerodynamic Stability Investigations of an Annular Compressor Cascade Based on Unsteady Pressure Measurements,* Proceedings of the 9th International Symposium on Unsteady Aerodynamics, Aeroacustics and Aeroelasticity of Turbomachines (ISUAAAT), 4–8 Sept 2000, Lyon, France, pp. 280–295

Bölcs, A. (1983). *A Test Facility for the Investigation of Steady and Unsteady Transonic Flows in Annular Cascades,* ASME Paper 83-GT-34

Buffum, D.H., Capece, V.R., King, A.J., and El-Aini, Y.M. (1998). *Oscillating Cascade Aerodynamics at Large Mean Incidence,* ASME Journal of Turbomachinery, Vol. 120, pp. 122–130

Carta, F.O. (1982). *An Experimental Investigation of Gapwise Periodicity and Unsteady Aerodynamic Response in an Oscillating Cascade. I – Experimental and Theoretical Results,* NASA Contractor Rep., CR-3513

Carstens, V. and Schmitt, S. (1999). *Comparison of Theoretical and Experimental Data for an Oscillating Transonic Compressor Cascade,* ASME Paper 99-GT-408

Hennings, H. and Belz, J. (1999). *Experimental Investigation of the Aerodynamic Stability of an Annular Compressor Cascade Performing Tuned Pitching Oscillations in Transonic Flow,* ASME Paper 99-GT-407

Kahl, G. and Hennings, H. (2000). *Computational Investigation of an Oscillating Compressor Cascade Experiment,* Proceedings of the 9th International Symposium on Unsteady Aerodynamics, Aeroacustics and Aeroelasticity of Turbomachines (ISUAAAT), 4–8 Sept 2000, Lyon, France, pp. 819–829

Körbächer, H. and Bölcs, A. (1996). *Steady-State and Time-Dependent Experimental Results of a NACA-3506 Cascade in an Annular Channel,* ASME Paper 96-GT-334

Körbächer, H. (1996). *Experimental Investigation of the Unsteady Flow in an Oscillating Annular Compressor Cascade,* Ph.D. Thesis, Swiss Federal Institute of Technology, Lausanne, Switzerland

Lepicovsky, J., MacFarland, E.R., Capece, V.R., and Hayden, J. (2002). *Unsteady Pressures in a Transonic Fan Cascade Due To a Single Oscillating Airfoil,* ASME Paper GT-2002-30312

Nowinski, M., and Panovsky, J. (1998). *Flutter Mechanisms in Low Pressure Turbine Blades,* ASME Paper 98-GT-573

Rottmeier, F. (2003). *Experimental Investigation of a Vibrating Axial Turbine Cascade in Presence of Upstream Generated Aerodynamic Guests,* Ph.D. Thesis, École Polytechnique Fédérale de Lausanne, Switzerland

Széchényi, E., and Girault, J.P. (1980). *A Study of Compressor Blade Stall Flutter in a Straight Cascade Wind-tunnel,* Symposium on Aeroelasticity in Turbomachines, Lausanne, Switzerland

Whitehead, D.S. (1987). *Classical Two-Dimensional Methods,* AGARD Manual on Aeroelasticity in Axial-Flow Turbomachines, AGARD-AG-298, Vol. 1, Chapter 3: Unsteady Turbomachinery Aerodynamics, M.F. Platzer and F.O. Carta, eds.